

# A Penning trap for g-factor measurements in highly charged ions by laser-microwave double-resonance spectroscopy

Nicolaas P. M. Brantjes · D. von Lindenfels · G. Birkel ·  
W. Quint · M. Vogel

Published online: 27 April 2011  
© Springer Science+Business Media B.V. 2011

**Abstract** Precise determination of bound-electron g-factors in heavy highly-charged ions (e.g.  $\text{Bi}^{82+}$ ,  $\text{U}^{91+}$ ) provides a stringent test of bound-state QED in extreme fields. With a laser-microwave double-resonance technique we will probe the microwave transitions between the Zeeman sub-levels of the hyperfine structure in highly charged ions. From this the bound electron g-factor  $g_J$  can be determined. We present the experimental progress of this novel method to measure the g-factor of the bound electron in highly charged ions.

**Keywords** QED · Charged ion · Heavy ion · Zeeman sublevel ·  
Double-resonance laser spectroscopy · Electronic g-factor

## 1 Introduction

In the present contribution, we report on recent experimental developments for tests of bound-state QED and/or determinations of fundamental constants via double-resonance laser spectroscopy of trapped hydrogen-like heavy ions [1]. We describe the experimental design and methods for accurate measurements of the  $g_F$ -factor of a high- $Z$  hydrogen-like ion (nucleus with non-vanishing spin).

Briefly, a mass- and charge-state selected ensemble of cooled and bunched highly charged ions from the HITRAP facility [2] will be injected into a cryogenic Penning

---

N. P. M. Brantjes (✉) · D. von Lindenfels · W. Quint · M. Vogel  
GSI, Planckstrasse 1, 64291 Darmstadt, Germany  
e-mail: klaasbrantjes@gmail.com

N. P. M. Brantjes · D. von Lindenfels · W. Quint  
University of Heidelberg, P.O. Box 10 57 60, 69047 Heidelberg, Germany

G. Birkel  
TU Darmstadt, Karolinenplatz 5, 64289 Darmstadt, Germany

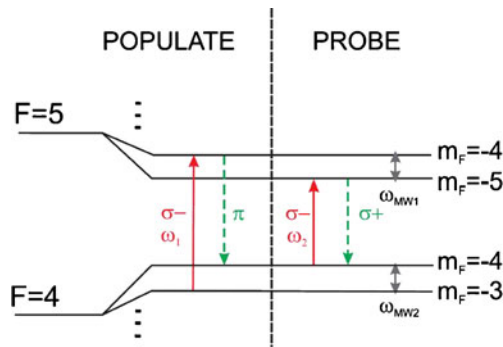


**Fig. 1** Scheme of the Zeeman-split hyperfine energy levels in the ground state of hydrogen-like Bismuth [6] with  $I = 9/2$ . Solid arrows indicate excitation lasers or microwaves. The level scheme allows a population of states with extremal  $m_F$  by optical pumping with polarised light. When microwave radiation at frequency  $\omega_{MW2}$  comes into resonance with the ( $F = 4, m_F = -4 \leftrightarrow -3$ ) transition the  $\sigma^+$  fluorescence disappears. Thus, by observation of the  $\sigma^+$ -fluorescence as a function of  $\omega_{MW2}$  the corresponding  $g_F$ -factor can be inferred

trap designed for laser and microwave spectroscopy. The ions will remain cooled at a motional temperature of about 4 K and will be excited by a combination of laser and microwave irradiation. The fluorescence signal will be detected axially. We consider a hydrogen-like ion of high nuclear charge, whose nucleus has a spin, in a magnetic field. In this case, every hyperfine level splits up into individual Zeeman sublevels. The double-resonance scheme (Fig. 1) in this case involves (1) microwave transitions among the Zeeman sublevels of the hyperfine level, and (2) laser-induced, optical transitions among the hyperfine levels of the hydrogen-like ion. With this technique, the  $g_F$ -factor of the electron can be determined. By combining the Zeeman splitting of two different hyperfine levels of the ion's ground state, the electronic and nuclear  $g$ -factors can be disentangled and measured independently with high accuracy.

## 2 Experimental techniques

### 2.1 Injection

At the GSI-HITRAP facility [2], heavy highly charged ions, such as H-like uranium, will be produced and decelerated. Bunches of up to  $10^5$  of these ions will be cooled to 4 K and transported to several experimental setups, such as the  $g$ -factor trap, at a transport energy of 5 keV/q. The length of a bunch is estimated to be roughly 25 cm.

The highly charged ions will be injected electro-statically into the magnetic field of the  $g$ -factor Penning trap, employing a scheme similar to that of the ISOLTRAP experiment [3]. A schematic overview of the injection line can be seen in Fig. 2. The simulated beam envelope is shown as well. The starting point of the ions in the simulations coincides with the focal point of an electrostatic bender leading to the  $g$ -factor trap. A retardation electrode at 2.5 kV and a pulsed drift tube at 4 kV slow down the ions to about 1 keV/q. While inside the pulsed drift tube, the potential will be ramped down to  $-0.7$  kV. The remaining part of the injection line, up to the Penning trap, maintains this potential. Three einzel-lenses provide focussing. With

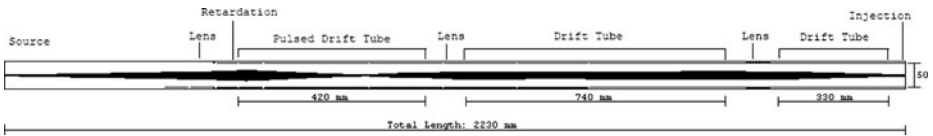


**Fig. 2** Schematic overview of the injection line. The beam envelope was simulated in Simion 8. The source of the ions was taken to be the focal point of the electrostatic bender

this configuration, H-like uranium ions can be focussed on a spot of less than 2 mm in diameter. After injection into the B-field, the ions will be strongly confined radially as they travel towards the trap. They will lose most of their remaining velocity against the ground potential of the trap. Trapping inside the Capture Trap will then happen at roughly 300 V.

## 2.2 Penning trap

The experiment will take place inside a Penning trap [4]. A magnetic field confines the ions in the radial direction while the electrostatic potential created by the cylindrical electrode structure of the trap confines the ions in the axial direction. The superconducting magnet provides a 7 T magnetic field with a precision of 10 ppm over the length of the Penning trap. Precision measurements can be performed inside a 1 cm<sup>3</sup> region of 0.1 ppm homogeneity. The electrode structure (Fig. 3) contains 19 electrodes and consists of three parts: an in-beam electron source, the ‘Capture Trap’ and a precision trap. For the electrodes we used high-purity copper to prevent deterioration of the magnetic field. Also, the electrodes were gold plated to prevent oxidation.

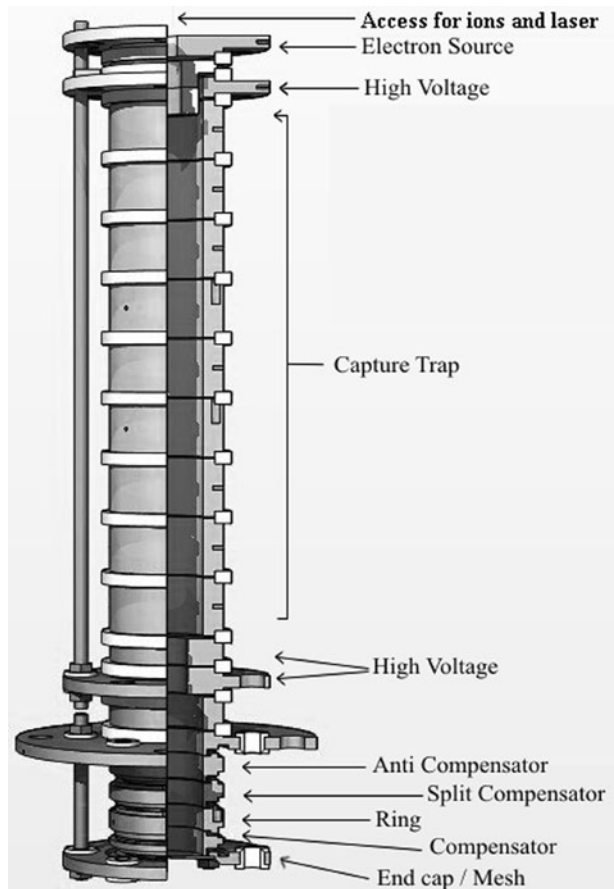
### 2.2.1 Capture trap

Ions coming from the HITRAP facility will be captured in the first section of the Penning trap. This ‘Capture Trap’ consists of two high-voltage electrodes for ion capture and nine low voltage electrodes designed for cooling and preparation of the ion cloud. The last high-voltage electrode, between the spectroscopy part of the trap and the Capture Trap, is split into two ring electrodes to allow smooth transport between the two traps. As an ion bunch enters the trap, it bounces back off the last high-voltage electrode. Before the bunch leaves the trap, the first high-voltage electrode is ramped up to trap the ions. The 9 low-voltage trap electrodes were designed such that the length is 1.203 times the diameter. With these dimensions, it becomes a mechanically compensated trap with a harmonic potential [4]. If these electrodes are at alternating but equal potentials, nine individual harmonic traps are created with virtual end caps in between. This will create enough freedom to manipulate a cloud of ions within the scope of our experiment.

### 2.2.2 Spectroscopy trap

The spectroscopy part of the Penning trap is based on a compensated closed Penning trap with five electrodes [4]. However, for our experiment we require an asymmetric electrode structure. On one side, where ions will enter the trap, the trap is ‘open’. On the opposite side, a closed configuration with a transparent mesh allows the close

**Fig. 3** g-Factor trap layout. Ions will be injected on the side of the electron source. Laser and microwave radiation can enter through this side as well. The Capture Trap will be used for cooling and preparation of the ions. The experiment itself will take place in the precision Penning trap below. Finally, fluorescence light can leave the trap through the mesh



proximity of a photon detector and thus a maximum solid angle for fluorescence photon detection. An accurate measurement of the axial oscillation frequency of the ion depends on a near-perfect harmonic electric potential at the centre of the trap. To this end, the spectroscopy part of the trap is artificially symmetrised by additional electrodes that replace the end cap on the injection side of the trap. These additional electrodes mimic a mirror trap on opposite potential. With careful tuning, there is a potential gradient between the real trap and the mirror trap where there would otherwise be an end cap.

### 2.3 Detection

An ion in a Penning trap induces an image current on the trap electrodes. We can measure this image current in a similar fashion to that of Schottky pick-up. Thus, the motional frequencies of this ion in the Penning trap can be determined. Typically the motional frequencies are between 100 kHz and 50 MHz. The magnitude of the image current induced for a single ion is in the fA region. Therefore, the detection circuit requires a low noise level. We can measure these signals with cryogenic amplification.

**Fig. 4** The superconducting axial resonator with a design inductance of 1.3 mH. It is a single coil with 225 windings of 0.125 mm thick NbTi wire. The resonator housing was made from gold-plated copper



### 2.3.1 Signal pick-up

Induced image currents will be picked up at several trap electrodes. In the spectroscopy part of the trap (Fig. 3), the compensator will be used to measure the axial frequency. One of the halves of the split compensator will be used for the cyclotron frequency.

In the capture section of the trap we will only detect the axial signal. This will be used to determine ion species and population. If we apply different potentials to the individual sub-traps, the axial frequency of each sub-trap changes and we can determine the ion-population for each individual sub-trap.

### 2.3.2 Resonator

First the ion signal is enhanced in an LC resonator circuit in resonance with the motional frequencies. An inductance in parallel with the parasitic capacitance of the trap ( $\sim 20$  pF) acts as a parallel resistance. To detect the axial frequency (between 300 kHz and 1 MHz) we will use a superconducting resonator (Fig. 4). The image current of a single ion in a Penning trap is very small ( $\sim$ fA). Therefore, the resonator circuit should have a high Q-value,  $Q = f_0/\Delta f$ , i.e. a high ratio of energy stored to energy lost per cycle [5]. For our superconducting resonator we expect values in excess of 5,000. This will act as an effective parallel resistance of a few MOhm. For a fA current we now achieve a signal of approximately 10 nV. At the same time, this parallel resistance resistively cools the ions in the trap. The cyclotron frequency can be determined with a non-superconducting coil. We studied the frequency behaviour of these resonators successfully in a room temperature prototype.

### 2.3.3 Amplification

In the second stage of the amplification we will use a cryogenic FET amplifier. The two main challenges for the transistor are charge carrier freeze-out and pink noise. The first challenge we overcome by using GaAs based transistors instead of Si transistors. For low frequencies, the noise of a FET is dominated by the  $1/f$ -noise, or pink noise. Above a certain frequency, the domain boundary, white noise dominates.

The domain boundary lies around 100 kHz, but it can be as high as 1 MHz. This coincides with the motional frequencies of the ion in the Penning trap. We tested several batches of transistors and we found a transistor with a domain boundary at 100 kHz and an input noise density of  $1.2 \text{ nV}/\sqrt{\text{Hz}}$ . Based on this transistor we designed a two-stage cryogenic amplifier with one amplification stage and one buffer stage. The voltage gain of the amplifier is roughly 4.

### 3 Summary

This experiment, using a double-resonance scheme with optical fluorescence photons as an observable for microwave transitions, will allow precise determinations of  $g$ -factors in the ions of interest. This renders possible sensitive tests of corresponding calculations of the transition energy and lifetime, especially of contributions coming from bound-state QED. We envisage measurements on an accuracy level of  $10^{-9}$  and beyond.

**Acknowledgements** We are thankful for the support of the DFG, BMBF, Helmholtzgemeinschaft and the IMPRS-QD, Heidelberg

### References

1. Quint, W., et al.: PRA **78**, 032517 (2008)
2. Kluge, H.-J., et al.: Adv. Quantum Chem. **53**, 83 (2007)
3. Bollen, G., et al.: NIM A **368**, 675–697 (1996)
4. Brown, L.S., Gabrielse, G.: Rev. Mod. Phys. **58**, 1 (1986)
5. Ulmer, S., et al.: Rev. Sci. Instr. **80**, 123302 (2009)
6. Moskovkin, D.L., et al.: Phys. Rev. A **70**, 032105 (2004)